Oximetry of Oxygen Supersaturated Solutions Using Nitroxides as EPR Probe

Alberto Moscatelli,[†] Thomas K. Chen,[‡] Steffen Jockusch,[†] Malcolm D. E. Forbes,[‡] Nicholas J. Turro,*[,†] and M. Francesca Ottaviani[§]

Department of Chemistry, Columbia University, 3000 Broadway, New York, New York 10027, Venable and Kenan Laboratories Department of Chemistry, CB# 3290 University of North Carolina, Chapel Hill, North Carolina 27599, and Institute of Chemical Sciences, University of Urbino, Piazza Rinascimento 6, 61029 Urbino, Italy

Received: November 8, 2005; In Final Form: February 14, 2006

The broadening of the three hyperfine EPR nitroxide lines in oxygen supersaturated solutions was examined. The solutions were supersaturated with oxygen either by thermal decomposition of 1,4-peroxy-1,4-dimethylnaphthalene or by pressurizing molecular oxygen above the sample solution. The linear relationship between the Lorentzian component of the line width and the O_2 concentration was proven to hold even when the hyperfine splitting is unresolved. In this region of line broadening, the requirement for spectral simulation is discussed.

Introduction

The EPR of nitroxides in dilute solutions of nonviscous solvents consists of three lines resulting from ^{14}N hyperfine coupling to the odd electron. Nitroxide EPR probes are widely used in chemistry and biology to monitor the chemical and physical properties of microenvironments. The EPR spectra of nitroxides are sensitive to variation in solvent viscosity, solvent polarity, temperature, molecular mobility, and molecular oxygen concentration.[1] In particular, the measurement of oxygen concentration inside cells, or biologic media in general, is very important in the study of oxidative processes, and nitroxide EPR provides a means for the direct measurements of oxygen concentration. Nitroxide EPR has been employed to analytically measure molecular oxygen concentrations.[2] It has been found that the concentration of oxygen influences the EPR spectrum of the nitroxides by homogeneously broadening the three hyperfine lines. The broadening effect of dissolved oxygen is the result of bimolecular spin exchange between the nitroxide radicals and the paramagnetic oxygen molecules.[3] The line widths of the nitroxide EPR spectra is related to the oxygen concentration through eq 1

$$\Delta H = \Delta H_0 + \frac{\hbar}{g_{O_2}\beta_e}\cdot\frac{2}{\sqrt{3}}\cdot k_e C_{O_2}\cdot 10^4 \qquad (1)$$

where g_{O_2} is the g factor of triplet oxygen, ΔH and ΔH_0 are the EPR line widths (measured in Gauss between the maximum and the minimum of the first derivative signal) in the presence and in the absence of oxygen, respectively, k_e is the rate constant for bimolecular spin exchange between oxygen molecules and nitroxide molecules, and C_{O_2} is the concentration of molecular oxygen. When there is a linear relationship between ΔH and C_{O_2} the EPR of nitroxides provides a valuable tool for the analytical determination of the oxygen concentration (oximetry).

SCHEME 1: Description of the System and Its Kinetic Constants[a]

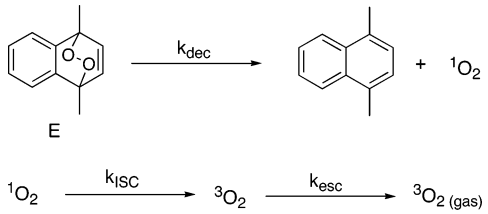

[a] Because the k_{ISC} is much smaller than the k_{dec}, the former is neglected. Therefore, the system is described by two kinetic contants: k_{dec} and k_{esc}.

However, as the amount of oxygen increases beyond a certain amount, the line broadening becomes so large that ΔH cannot be measured directly from the experimental spectra, because of overlap of the three nitroxide lines; this effect leads to unresolved hyperfine lines, thus introducing a Gaussian component (inhomogeneous broadening). Only the Lorentzian component is proportional to the oxygen concentration and the task of extracting it from inhomogeneously broadened spectra often requires sophisticated simulation programs.

In this paper, we investigate the possibility of oximetry in a previously unexplored region of very high oxygen concentrations, i.e., where the hyperfine structure (due to ^{14}N nucleus) of the nitroxide spectrum is completely unresolved and the standard methods of analyzing the three-line spectrum fail. High concentrations of molecular oxygen are achieved by generating supersaturated solutions of oxygen through the thermal decomposition of 1,4-peroxy-1,4-dimethylnaphthalene (E, Scheme 1). This novel method can produce metastable supersaturated solutions of molecular triplet oxygen that cause line broadening of the nitroxide EPR well above that which can be produced by the equilibrium concentrations of oxygen available at 1 atm pressure. The goal of this research is to determine experimentally whether the Lorentzian component of nitroxide line widths is still linearly proportional to the molecular oxygen concentration in this high concentration region. The use of endoperoxides as singlet ($^1\Delta$) oxygen carriers, releasers, and trappers[3] in cancer therapy could make this study useful for biomedical applica-

* To whom correspondence should be addressed. E-mail: njt3@columbia.edu.
[†] Columbia University.
[‡] University of North Carolina.
[§] University of Urbino.

10.1021/jp056458a CCC: $33.50
Published on Web 03/17/2006

tions.[4] Moreover, as an experimental check, we produced solutions with high equilibrium concentrations of oxygen in a second and alternative way, by pressurizing molecular oxygen above the sample solution.

Experimental Section

4-Oxo-TEMPO was purchased from Aldrich and was used without further purification. 1,4-Peroxy-1,4-dimethylnaphthalene (E) was synthesized following a standard procedure.[5]

For the CW-EPR measurements (Bruker EMX; X-band spectrometer), 300 μL of a solution of a predetermined concentration of E and 4-oxo-TEMPO in benzene was prepared. Then 250 μL of the solution was transferred to a 3-mm ID quartz tube for the EPR analysis. The procedure was carried out in an ice bath to avoid the thermal decomposition of E before the insertion of the sample tube inside the EPR cavity at the selected temperature. The temperature of the cavity was kept constant by a temperature controller (Bruker BTV3000) with an accuracy of $\pm$0.1 K. The acquisition parameters were such to provide a relatively fast scan (around 40 s) and an acceptable field resolution (typically 300 G sweep and 1024 points). The incident microwave power was 0.2 mW.

The pressurized EPR apparatus has been described in detail previously,[6] and the modifications for high pressure are detailed in a separate publication.[7] Briefly, spectra were recorded on a Varian E-line X-band (9.5 GHz) EPR console, bridge modified with a low noise GaAs FET microwave amplifier (25 dB gain) for better sensitivity. The microwave power incident on the samples was 0.2 mW. High-pressure solutions were circulated through a quartz flow cell of 9-mm outside diameter, 2-mm inside diameter using a specially modified micropump with a sapphire shaft. The quartz sample tube was epoxied to stainless steel pressurizing heads and centered in a home-built cylindrical TE_{011} microwave cavity (silver helix bound to a quartz support wall). The exterior of the cavity was equipped with a set of standard Varian E-line Century Series modulation coils. The flow system was routinely pressure-tested to 200 bar, and experiments were run below 180 bar.

Safety Note. Initial pressurization of such flow systems should always be carried out with full-face protection. We also recommend using a plexiglass safety shield around the sample cell/resonator assembly at all times when the pressure is above ambient. On occasion when ramping up the pressure, we have experienced the shattering of sample cells or failure of the epoxy seals between the quartz tube and the stainless steel pressurizing heads.

Spectra Simulation Strategy. The computation of all the spectra at different temperatures and oxygen concentrations was performed by means of established procedures.[8] The g_{ii} tensor components for the coupling between the electron spin and the magnetic field were obtained from the literature ($g_{xx} = 2.0104$, $g_{yy} = 2.0074$, $g_{zz} = 2.0026$);[9] the A_{ii} components for the coupling between the electron spin and the ^{14}N nuclear spin ($A_{xx} = 5.0$ G, $A_{yy} = 5.0$ G, $A_{zz} = 33.5$ G) and the correlation time for the rotational diffusion motion ($\tau = 1 \times 10^{-11}$ s) were obtained by simulating the spectrum under air-equilibrated conditions and held constant during the simulations. For the computations for each series of measurements, the line width was the only parameter that was changed over time.

Simulation of a set of spectra was initiated by taking the spectrum of the longest time (equilibrium oxygen situation) to make sure that the three hyperfine lines did not overlap. Under these conditions, the EPR lines are purely Lorentizan. Using this spectrum as a standard for the computations, we employed the best-fit parameters as a starting point for the next spectrum going to shorter times.

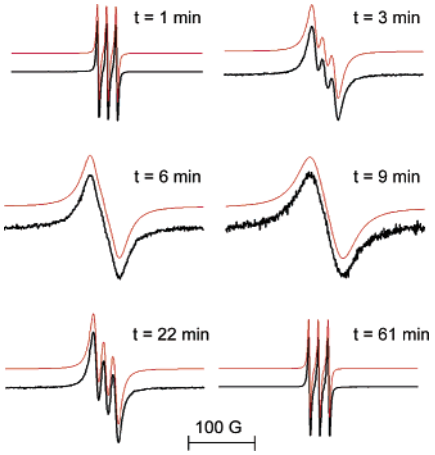

Figure 1. EPR spectra of 4-oxo-TEMPO (0.6 mM) in benzene at 330 K at different times. Endoperoxide (initial concentration = 130 mM) decomposition begins ($t = 0$) when the sample is put into the heated cavity. Black lines: experimental spectra; red lines: simulated spectra.

A Gaussian contribution to the line width needs to be added to the computation when the three hyperfine lines broaden and merge into a single broad line. This computation allowed us to extract the Lorentzian component (ΔH^L) and plot it as a physical parameter for the spin−spin exchange frequency.

Results and Discussion

Benzene solutions containing different concentrations of 1,4-peroxy-1,4-dimethylnaphthalene (E) (80, 130, and 200 mM) and 4-oxo-Tempo (0.6 mM) were heated inside the EPR cavity to different temperatures (298, 314, and 330 K). A high concentration of 4-oxo-TEMPO (0.6 mM) was selected to achieve a strong EPR signal intensity, but the concentration was low enough to prevent intermolecular spin−spin interactions, which would lead to changes in the signal shape.

Figure 1 shows, as an example, the EPR experimental (full lines) and computed (dashed lines) spectra of 4-oxo-TEMPO in benzene solution containing E at an initial concentration of 130 mM. The spectra in the figure were recorded at different times after insertion of the sample ($t = 0$) into the thermostated EPR cavity at 330 K. Once in the cavity, the endoperoxide starts decomposing into 1,4-dimethylnaphthalene and oxygen following the reaction sequence shown in Scheme 1.

The initial increase in line width reflects triplet oxygen formation from thermal decomposition of E. According to our simulations (vide infra), the maximum amount of triplet oxygen placed into solution by the complete decomposition of 130 mM of E is reached after 10 min and is almost 100 mM at 1 atm (with ambient pressure above the sample), far exceeding the equilibrium concentration of oxygen at 1 atm in benzene at 330 K (9.0 mM[10]). Because the sample is not stirred, a supersaturated solution of oxygen is created by the decomposition of E. The system will approach equilibrium on a time scale that depends on several factors such as the rate of production of molecular oxygen and the rate of escape of the molecular oxygen to the atmosphere above the liquid in the sample tube. When the system is supersaturated with oxygen, the EPR of 4-oxo-TEMPO is severely broadened, resulting in a single line. As the system approaches equilibrium, the EPR of 4-oxo-TEMPO approaches the standard three-line spectrum that is expected at the equilibrium concentration of oxygen. A simple model for the key rate constants is provided in Scheme 1: (a) the rate

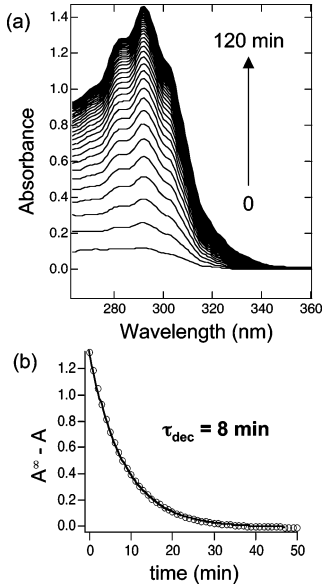

Figure 2. (a) UV−vis spectra of benzene solutions containing E after different heating times at 330 K. (b) Difference between the absorbance at 292 nm (corresponding to the generated 1,4-dimethyl naphthalene) at infinite time (120 min) and the absorbance at time *t* (open circles) vs time; first-order decay fit (solid line).

k_{dec}, for the endoperoxide decomposition; (b) the rate k_{ISC}, for the intersystem crossing of singlet ($^1\Delta$) to triplet ($^3\Sigma$) oxygen; (c) the rate k_{esc}, for the release of oxygen from the sample tube into the gas phase above the sample.

The lifetime of singlet ($^1\Delta$) oxygen in pure benzene at room temperature is 30 μs, whereas in pure d_6-benzene it is 681 μs.[11] These times are much shorter than the overall time scale to reach the equilibrium saturation shown in Figure 1, which is in the order of tens of minutes. We therefore expect a negligible contribution from k_{ISC} to the observed kinetics. To verify the expectation, we performed the equivalent EPR experiments in normal benzene and d_6-benzene. We reasoned that if the kinetics had been determined by k_{ISC}, then we would have observed a large difference in the kinetics in normal benzene and d_6-benzene. However, there was no experimental difference in the line width evolution over time for samples run in normal benzene or in d_6-benzene. We conclude that we can neglect k_{ISC} from the description of the kinetics of the system.

The value of k_{dec} was determined by UV−vis spectroscopy. The decomposition product of E, 1,4-dimethylnaphthalene, shows a strong absorption at 292 nm, whereas E is practically transparent at 292 nm. The absorption signal at 292 nm of the samples containing E increases in intensity over time, as shown in Figure 2a. The absorbance at 292 nm at any given time minus the absorbance at 292 nm at infinite time is directly proportional to the concentration of E. The exponential fit of these subtracted absorption values (Figure 2b) yields $k_{dec} = 2.1 \times 10^{-3}$ s^{-1}, corresponding to a lifetime of E of $\tau_{dec} = 8$ min.

The value of k_{esc} depends on a number of factors, including the size and geometry of the EPR tube. In the present study, we used EPR tubes of fixed diameter (3 mm ID) and fixed length with a 250 μL of solution. These sizes allowed easy measurement of the kinetics of oxygen depletion from the solution into the gas phase above the sample as the system approaches an equilibrium concentration of oxygen. The use of smaller or larger tubes was found to release oxygen from the sample too slowly or too rapidly for the convenience of EPR analysis. The value of k_{esc} was estimated by saturating a 0.6 mM 4-oxo-TEMPO solution in benzene with oxygen by

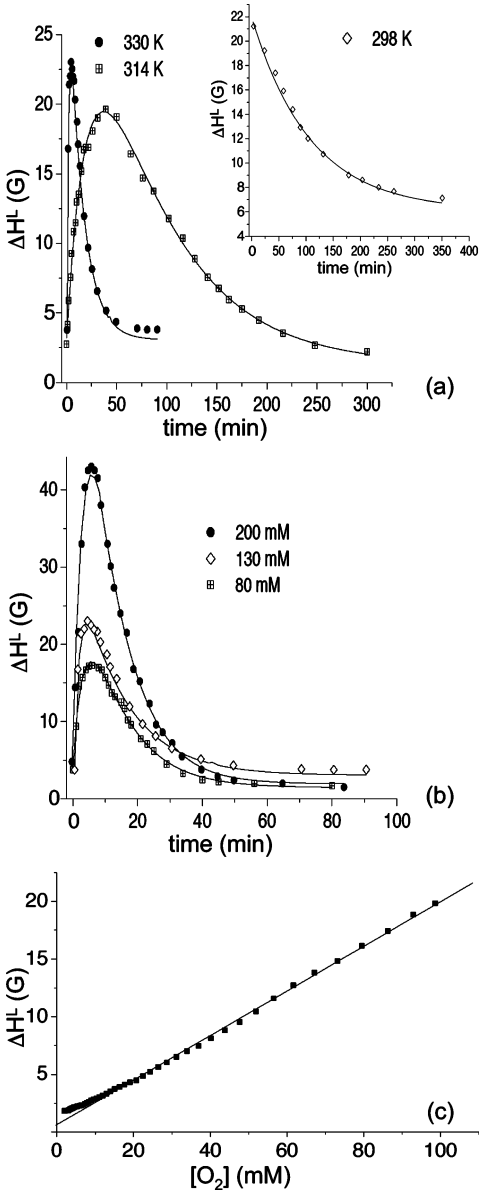

Figure 3. (a) ΔH^L_{pp} extracted from spectral simulation vs time at different temperatures ([E] = 130 mM); the solid lines are the double exponential fits to determine k_{dec} and k_{esc} (reported in Table 1). Insert: ΔH^L_{pp} vs time at a temperature of 298 K. For this experiment, the sample was heated to 330 K for 8 min and then quickly cooled to 298 K. (b) ΔH^L_{pp} extracted from spectral simulation versus time at three different concentrations of E (constant temperature at 330 K); the solid lines are the double exponential fits to determine k_{dec} and k_{esc} (reported in Table 1); (c) Correlation between ΔH^L_{pp} and oxygen concentration for the sample at 330 K and [E] = 130 mM.

bubbling O_2 at 273 K and measuring the variation in 4-oxo-TEMPO line width as the O_2 escapes from the solution at 330 K and approaches equilibrium with the atmosphere above the sample. This method is essentially oximetry by EPR, since the hyperfine structure of the spectrum is still apparent and no significant Gaussian contribution was needed to simulate the spectra. From these measurements, the value of $k_{esc} = 1.1 \times 10^{-3}$ s^{-1}, corresponding to $\tau_{esc} = 15$ min, was determined.

Figure 3a shows the behavior of ΔH^L (obtained from simulations) versus time. The best fit was obtained using a double exponential function, as expected from our kinetic equations. The decay times, corresponding to the E decomposition and O_2 escape, are $\tau_{dec} = 8$ min and $\tau_{esc} = 14$ min, respectively, and are in a very good agreement with the decay

TABLE 1: Kinetic Parameters Used to Simulate the Curves in Figure 3a,b[a]

[E] (mM)	T (K)	τ_{dec} (min)	τ_{esc} (min)
200	330	7	11
80	330	8	13
130	330	8	14
130	314	22	74
130	298	—[b]	110

[a] See text for details. [b] This sample was heated to 330 K for fast oxygen release and then quickly cooled to 298 K for τ_{esc} measurements. Therefore, τ_{dec} was not determined.

times obtained from the independent measurement described above. The knowledge of the kinetic constants allowed us to solve the first-order differential equations for our system and calculate the oxygen concentration at any instant. In Figure 3c, the O_2 concentration is plotted versus ΔH^L to obtain a linear correlation also for an oxygen concentration range in which the hyperfine structure is unresolved, a situation for which the oxygen concentration is higher than that usually used for oximetry studies by EPR. In fact, using endoperoxide decomposition (at 130 mM and 330 K) as a source of dissolved oxygen, an oxygen concentration in the order of ~100 mM was achieved after $t = 10$ min. This value is 50 times higher than the value for an air-saturated benzene solution (2.0 mM), and about 10 times higher than in oxygen-saturated O_2 solution (9.0 mM) at the same pressure and temperature.[9]

The same procedure was repeated for different E concentrations and different temperatures. Figure 3b shows also the variation over time of the Lorentzian line width for the higher (200 mM) and the lower (80 mM) E concentrations. As expected, on the basis of the analysis reported above, the higher the E concentration, the higher the oxygen concentration and the larger the line broadening. However, as obtained from the biexponential fitting (full lines in the plots), the two kinetics for E decomposition, τ_{dec}, and for oxygen release, τ_{esc}, do not show any significant difference with respect to the E concentration (see also Table 1).

A different situation was found at temperatures lower than 330 K, also shown in the graph in Figure 3a for the sample at [E] = 130 mM and $T = 314$ K. With decreasing temperature, the line broadening diminished. This is expected because the decomposition of the endoperoxide is significantly slower at reduced temperatures. Therefore, the achieved maximum oxygen concentration is much lower. The fitting of the Lorentzian component of the line width versus time revealed that the lifetimes of the processes are much longer ($\tau_{dec} = 22$ min and $\tau_{esc} = 74$ min) compared to higher temperatures (see also Table 1). A further decrease of the temperature (e.g., 298 K) slowed both processes, E decomposition and oxygen escape, and fitting of the biexponential line width did not yield reliable lifetimes.

To avoid this problem, we followed a different procedure for the analysis of the oxygen release at room temperature (298 K): first, the sample was heated to 330 K for 8 min. On the basis of the results described above, the molecular oxygen concentration is maximum at that time at 330 K. Then, the temperature was rapidly decreased to 298 K and the process of oxygen release was followed over time in the EPR cavity, assuming as $t = 0$ the time at which the cavity reached 298 K. The decrease of the of Lorentian line width as a function of time is also reported in Figure 3a (insert). This experimental method reduced the biexponential kinetics (rise + decay) to a simpler monoexponential decay kinetics and yielded $\tau_{esc} = 110$ min, the oxygen release kinetics at room temperature.

It was of interest to determine if the simple method using

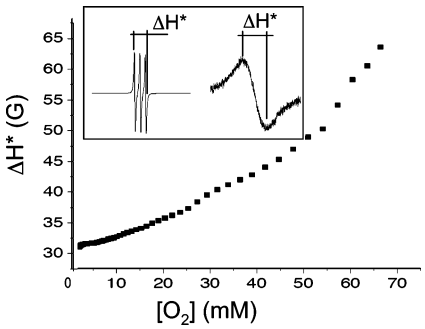

Figure 4. Plot of the experimental parameter (ΔH^*) versus O_2 concentration ([4-oxo-TEMPO] = 0.6 mM; [E] = 130 mM; $T = 330$ K); Inset: experimental parameter ΔH^* is the distance between the first maximum and the last minimum of the EPR spectra. Note that ΔH^* is the experimental line width when the hyperfine splitting is no longer resolved.

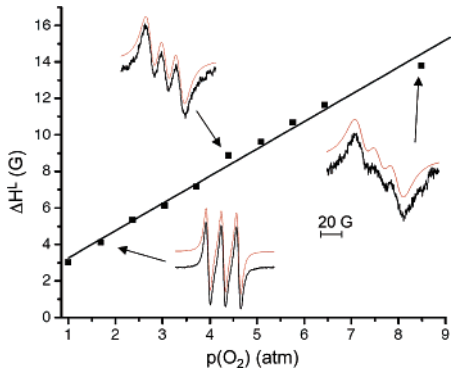

Figure 5. Plot of ΔH^L vs the concentration of oxygen for the pressurized experiment in benzene. Black lines: experimental spectra; red lines: simulated spectra.

spectral parameters, which could be directly extracted from the spectra, could produce a reliable correlation with the oxygen concentration and thereby eliminate the need for a simulation. Such a direct spectral parameter is the value of ΔH^*, the distance between the first maximum and the last minimum of the spectrum (see inset of Figure 4). The results in Figure 4 show a nonlinear relationship. The lack of a linear correlation is due to the Gaussian contribution to ΔH^*. However, if a calibration curve can be obtained, the simple method, using ΔH^*, can be used to perform oximetry.

Because the creation of a supersatured solution is a novel procedure for the exploration of the EPR oximetry at very high concentrations of oxygen, it is important to verify the concept with an independent method. Such a method is available by investigation of the EPR of 4-oxo-TEMPO under varying high pressures of oxygen, which allowed an increase in the concentration of dissolved oxygen *at equilibrium*. The relationship between ΔH^L and oxygen concentration was therefore investigated in an EPR cell that allows the pressure of oxygen above the sample to be varied. In this case, the concentration of O_2 was directly measured through its pressure.

The cell employed in the high-pressure experiments was flushed with N_2 overnight to purge excess O_2 and to dry the system. The pressurized EPR system consists of a small reservoir (~15 mL), pressure gauges, relief valves, a high pressure pump, and connection tubing, all of which were filled with solution during the experiment. In advance of each run, the reservoir was charged with a solution of nitroxide and the pump was turned on to fill the system. This pumping was normally carried out for 3 to 5 min, to assist in achieving an equilibrium distribution of O_2 throughout the solution prior to data collection.

The oxygen pressure was increased from 1 to 8.5 atm pressure, over the course of each sample run. Experiments at lower pressures were run first to avoid the possibility of initially saturating the solution with O_2. The EPR spectra were simulated, and the Lorentzian component was plotted versus the oxygen pressure (Figure 5). A linear relationship between ΔH^L and the pressure of oxygen (concentration of dissolved oxygen) was observed even when the three hyperfine lines merges, as in the case of E decomposition. This result confirms that the dominant feature influencing the EPR spectra is the dissolved oxygen concentration.

Conclusions

We have demonstrated that it is possible to use the line width of nitroxides for oximetry by EPR even in regions of very high O_2 concentrations where the three hyperfine lines of nitroxides are not resolved. In this region of strong spectral broadening, a Gaussian component plays a significant role in determining the form of the spectra. It is therefore essential for oximetry measurements to extract the Lorentzian component, which is the parameter that is proportional to the O_2 concentration. Spectral simulations offer a valuable method for the extraction of the Lorentzian component. High concentrations of oxygen in benzene or aromatic solvents, well above those achievable at equilibrium at a given temperature and 1 atm, can be achieved employing the decomposition of an endoperoxide as a source of molecular oxygen or by increasing the pressure of oxygen above the sample to values greater than 1 atm.

Acknowledgment. The authors at Columbia University thank the National Science Foundation (Grant CHE-04-15516) for generous support of this research.

M.D.E.F. and T.K.C. thank the National Science Foundation for continued support of their program through Grant No. CHE-0213516 and instrumentation Grant No. CHE-9709037. This work also received partial support from the STC Program of the National Science Foundation under Agreement No. CHE-9876674.

References and Notes

(1) Seelig, J.; Smith I. C. P.; Butler K. W.; Griffith, O. H.; Jost P. C.; McConnell H. M. In *Spin Labeling: Theory and Applications*; Berliner, L. J., Ed.; Academic Press: New York, 1976; Chapters 10−13.

(2) Povich M. J. *Anal. Chem.* **1975**, *47*, 346.

(3) For a review on endoperoxides as oxygen carriers, see: Aubry, J.-M.; Pierlot, C.; Rigaudy, J.; Schmidt, R. *Acc. Chem. Res.* **2003**, *36*, 668.

(4) For recent reviews on oximetry by EPR in biology and medicine, see: (a) Grucker D. *Prog. Nucl. Magn. Res*. **2000**, *36*, 241. (b) Swartz H. M.; Khan, N.; Buckey, J.; Comi, R.; Gould, L.; Grinberg, O.; Hartford, A.; Hopf, H.; Hou, H.; Hug, E.; Iwasaki, A.; Lesniewski, P.; Salikhov, I.; Walczak, T. *NMR Biomed.* **2004**, *17*, 335.

(5) Denny, R. W.; Nickon, A. *Org. React.* **1973**, *20*, 185.

(6) Forbes, M. D. E. *Photochem. Photobiol.* **1997**, *65*, 73.

(7) Dukes, K. E.; Harbron, E. J.; Forbes, M. D. E.; DeSimone, J. M. *Rev. Sci. Instrum.* **1997**, *68*, 2505.

(8) Budil, D. E.; Lee, S.; Saxena, S.; Freed, J. H. *J. Magn. Res. A* **1996**, *120*, 155.

(9) *Spin Labeling: Theory and Applications;* Berliner, L. J., Ed.; Academic Press: New York, 1976; Appendix II.

(10) Estimated value from Battino, R. *Oxygen and Ozone*, Solubility Data Series, Vol. 7; Pergamon: New York, 1981; p. 250.

(11) Schmidt, R.; Afshari, E. *Ber. Bunsen-Ges. Phys. Chem*. **1992**, *96*, 788.